Passivity of metals and metallic alloys
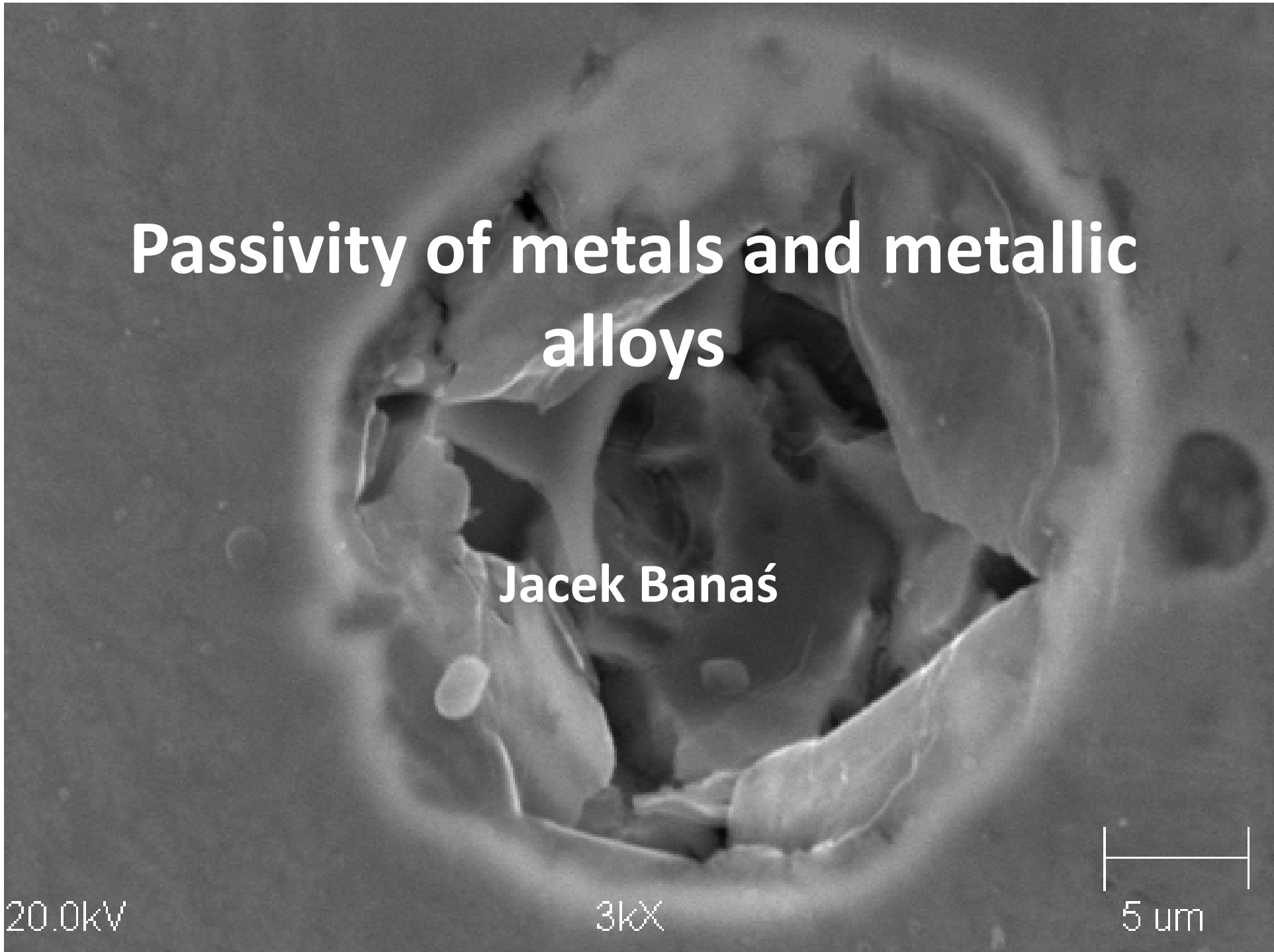
Jacek Banaś

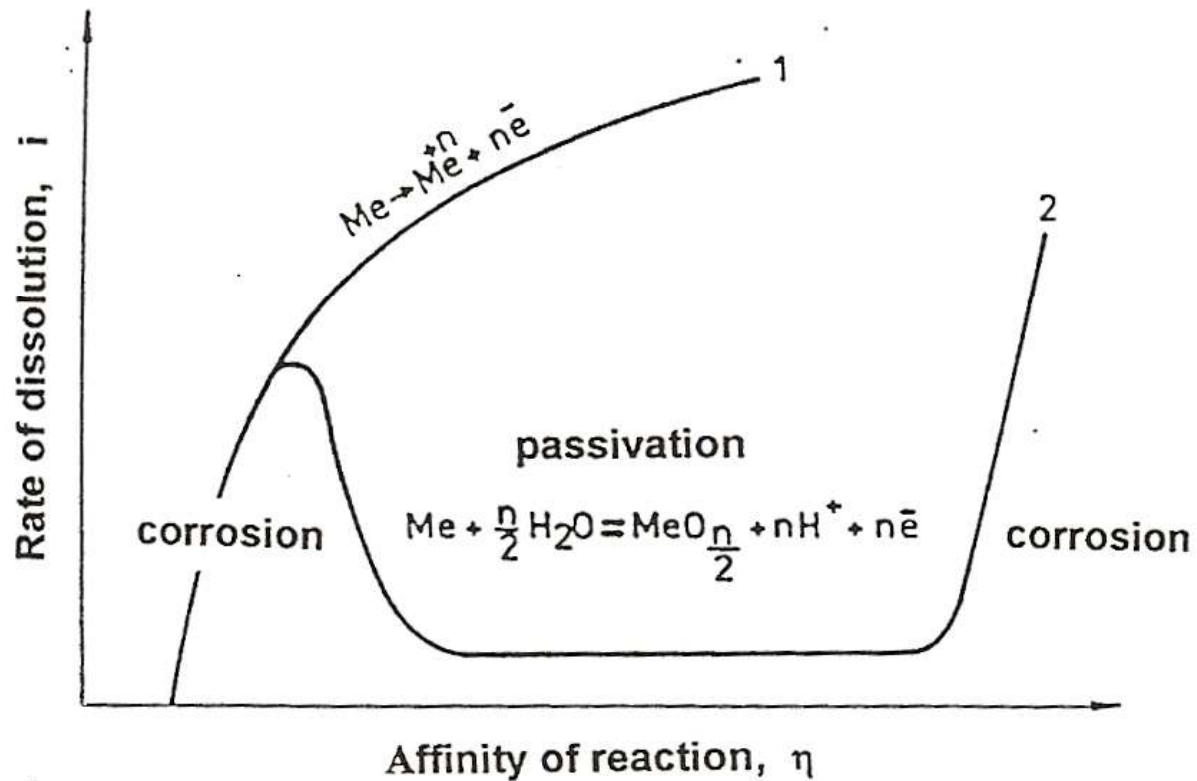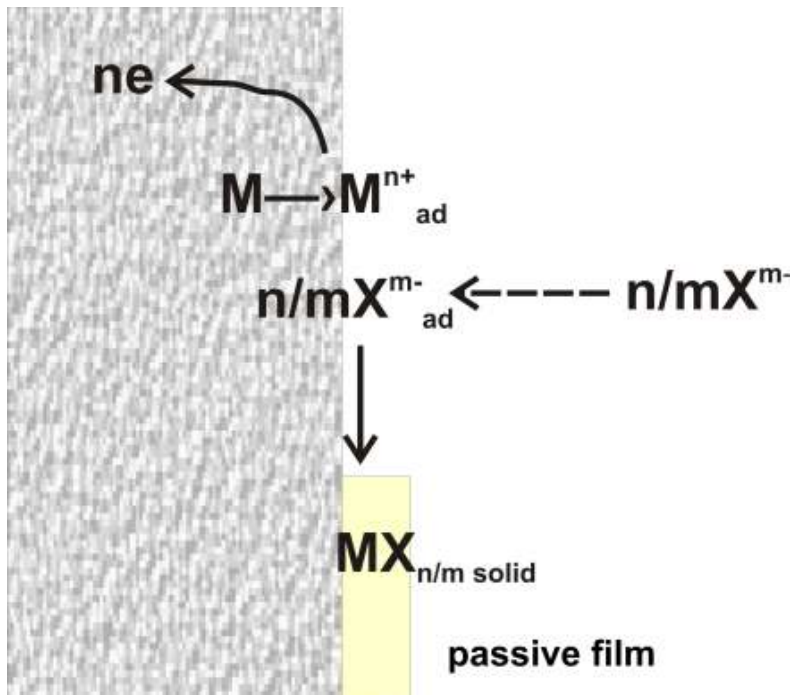20.0kV   3kX   5 um

Wagner definition of passivation

Metal is passive when its corrosion in course of chemical or electrochemical reaction is lower at higher affinity of reaction than at lower affinity of chemical or electrochemical process
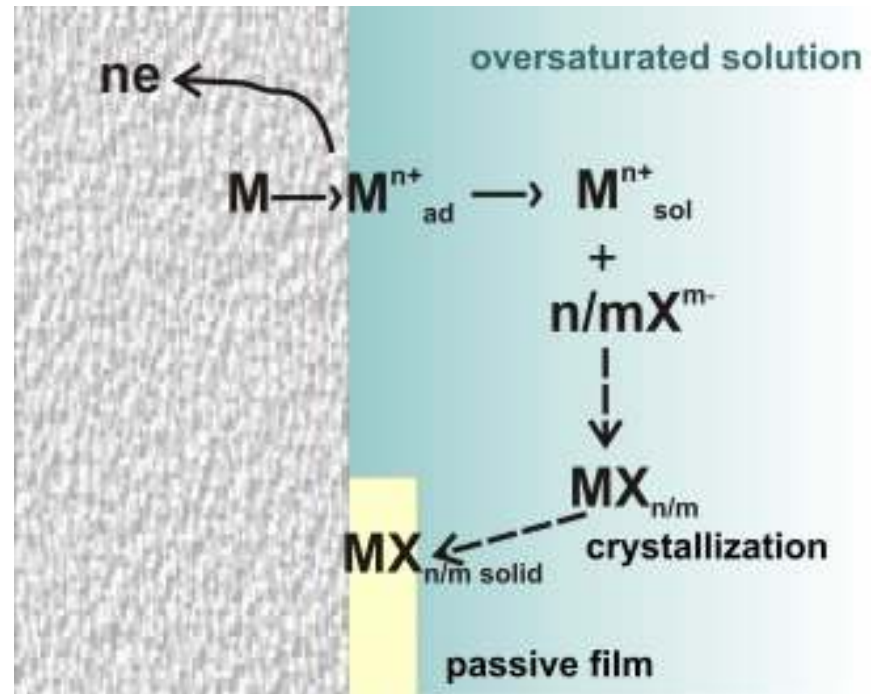

*C. Wagner: Corrosion Science 5, 751 (1965)*

Mechanism of passivation

$$Me + n/m \, X^{-m} \rightarrow MeX_{n/m} + ne$$

solid state reaction

precipitation mechanism

Oxide passivation

Water molecule is a source of oxygen

$$Ni + H_2O \rightarrow NiO + 2H^+ + 2e$$
$$2Cr + 3H_2O \rightarrow Cr_2O_3 + 6H^+ + 6e$$

In anhydrous environments other molecules can be a source of oxygen (undissociated molecules of oxy-acids: H_2SO_4, H_3PO_4, HNO_3, HCOOH)

$$Cr + H_2SO_4 \rightarrow CrHSO_{4\,ad} + H^+ + e$$
$$CrHSO_4 \rightarrow CrOOH + SO_2$$
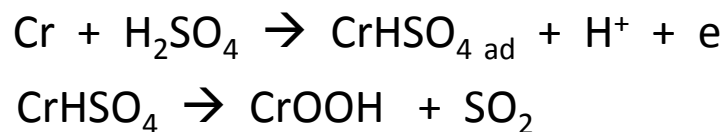
B. Stypuła, J. Banaś: Electrochim. Acta 38, 2309 (1993)

$$Fe + 2HCOOH \rightarrow FeOOH + 2CO + 3H^+ + 2e$$

J. Banaś, B. Mazurkiewicz, W. Solarski, K. Banas: Material Science Forum Vol.185-188, 845 (1995),

Mechanism of passivation in aqueous solutions

$$Me^{2+} + H_2O$$

$$+ H^+$$

dissolution

$$MeOH^+ + e^-$$

$$Me + H_2O \rightarrow Me(H_2O)_{ad} \rightarrow MeOH_{ad} + H^+ + e^-$$

$$+ H_2O$$

intermediate

$$Me(OH)_2 + H^+ + e^-$$

passivation

$$MeO + H_2O$$
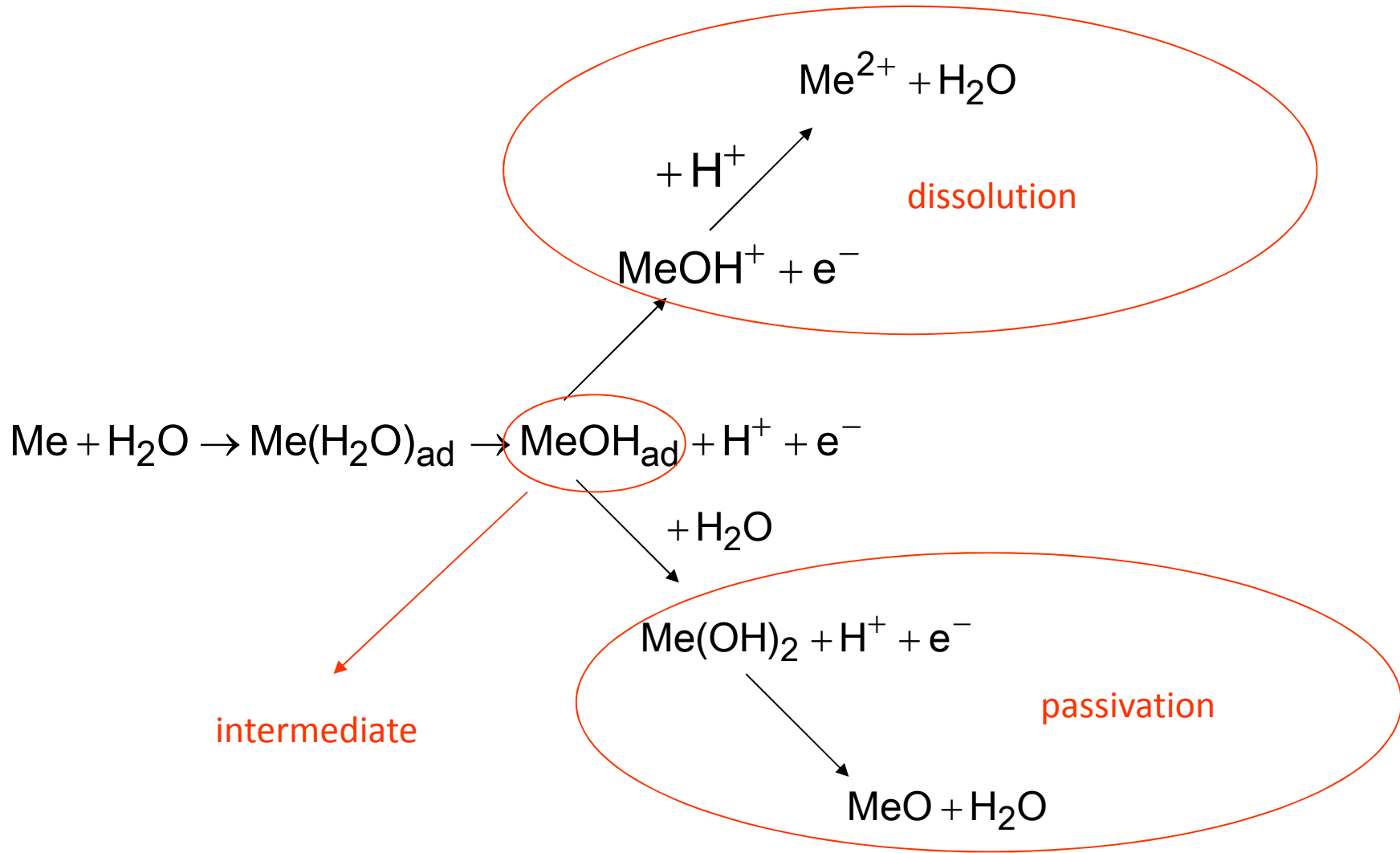
K. Schwabe, S. Hermann, W. Oelssner: Passivity of Metals, Proc. of the Fourth Int. Symp. on Passivity, ed. by R.F. Frankenthal and J. Kruger, N.Y. 1977,

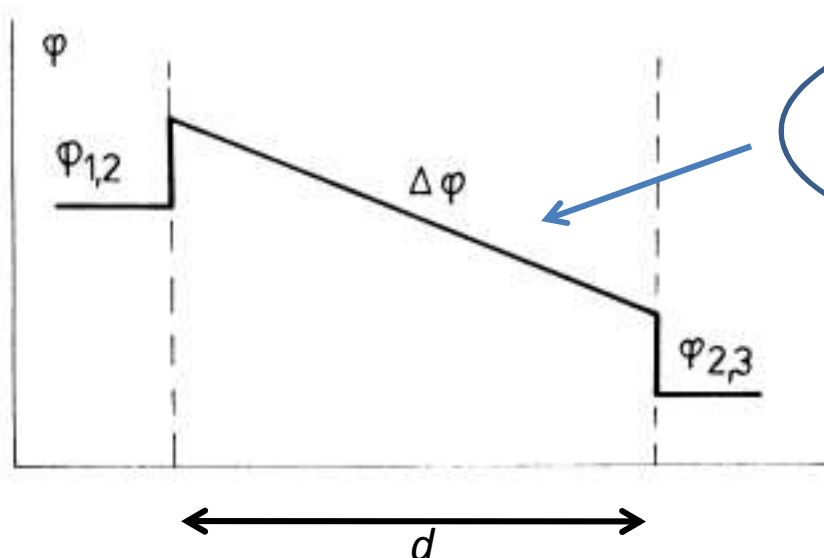# Mechanism of iron passivation in aqueous solutions
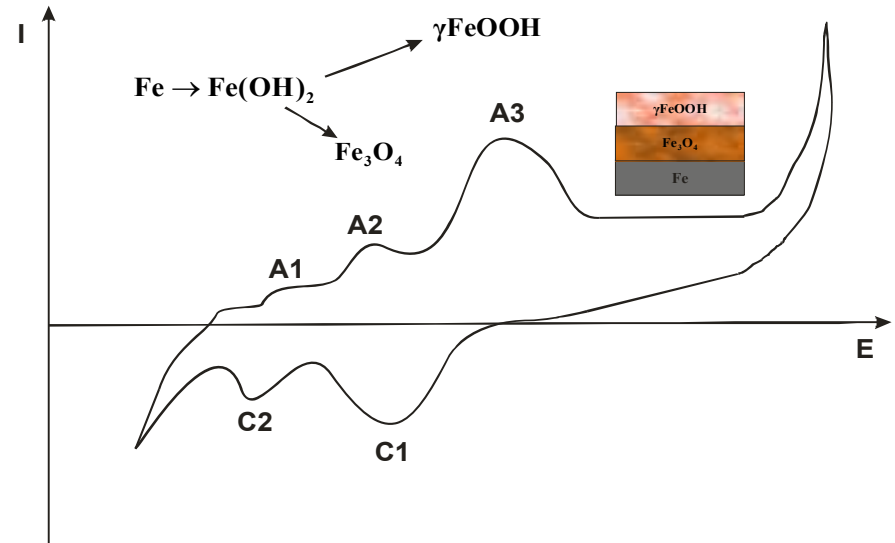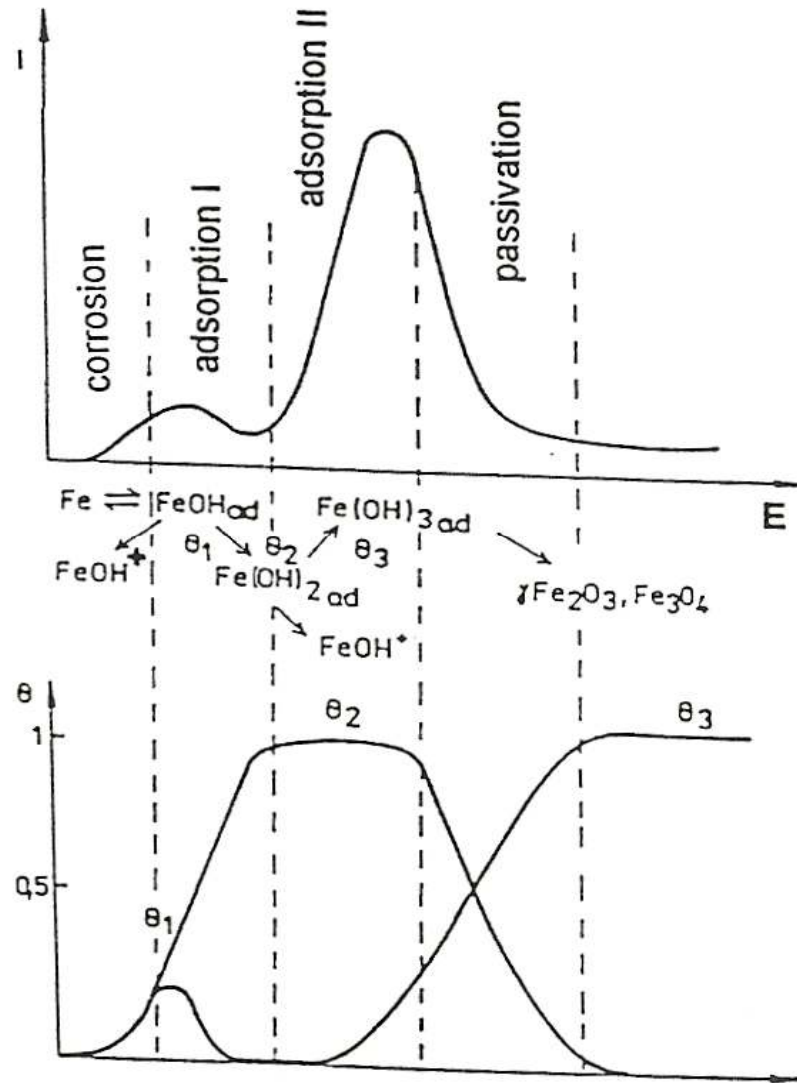
Cyclic voltamperometric curve of iron polarization in neutral environment

W.J. Lorenz, K. E. Heusler in Corrosion Mechanisms ed. Marcel Dekker Inc. N. York 1987

High field mechanism (hfm) of oxide growth

Electric field: $$E = \frac{\Delta\Phi}{d} = \frac{\Phi_{1/2} - \Phi_{2/3}}{d}$$

Electric field is a driving force for growth of oxide film. The anodic current related to growth of the film is an exponential function of electric field:
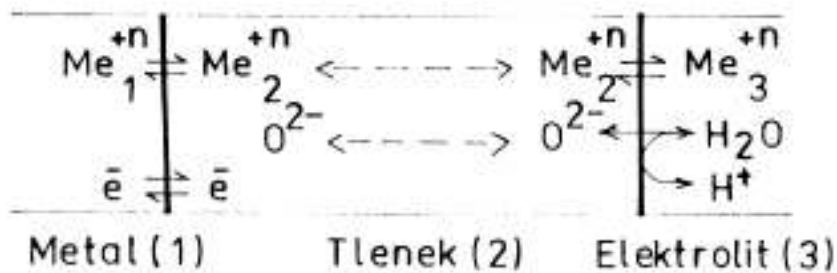
$$i = i^0 \exp\left(\frac{\beta\Delta\Phi}{d}\right)$$

$$i_0 = \rho\,\chi e v \exp\left(\frac{-W}{RT}\right)$$

$$\beta = \frac{\chi a F}{RT}$$

Metal (1)   Oxide (2)   Electrolyte (3)

K.J. Vetter: *Elektrochemische Kinetik*, Springer Verlag 1962

High field mechanism (hfm) of oxide growth

$$i = i^0 \exp\left(\frac{\beta \Delta \Phi}{d}\right)$$

$$i_0 = \rho\, \chi e \nu \exp\left(\frac{-Q}{RT}\right)$$
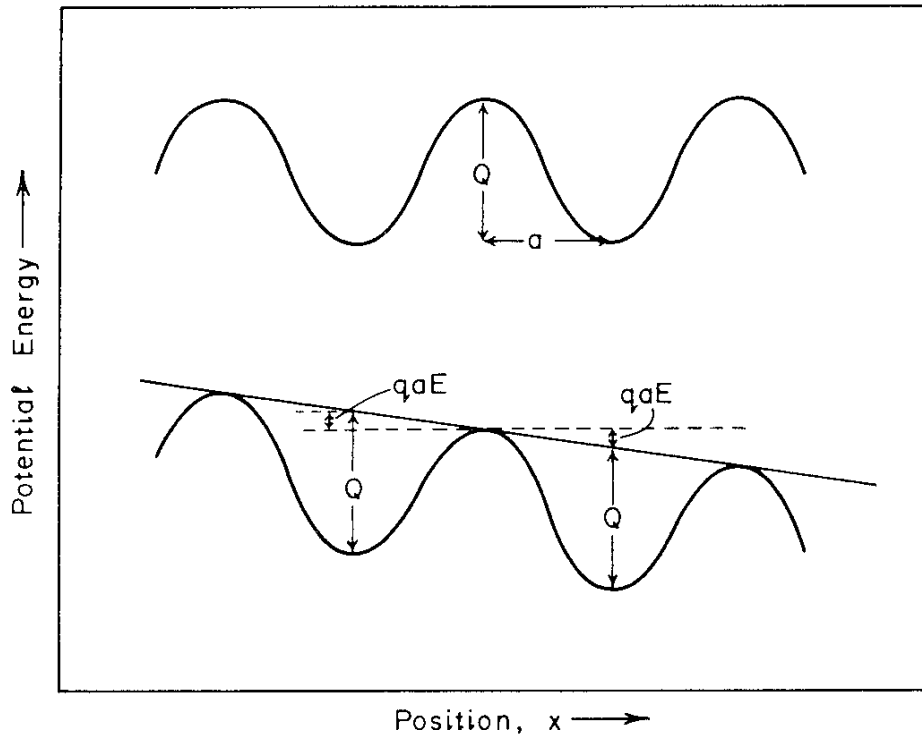
$$\beta = \frac{\chi aF}{RT}$$

ρ - surface density of adatoms (mobile atoms)

Xe - charge of the ion

ν – oscillation frequency of metal atoms in crystalline lattice of oxide

Q – activation energy of jump of ion from one to other position
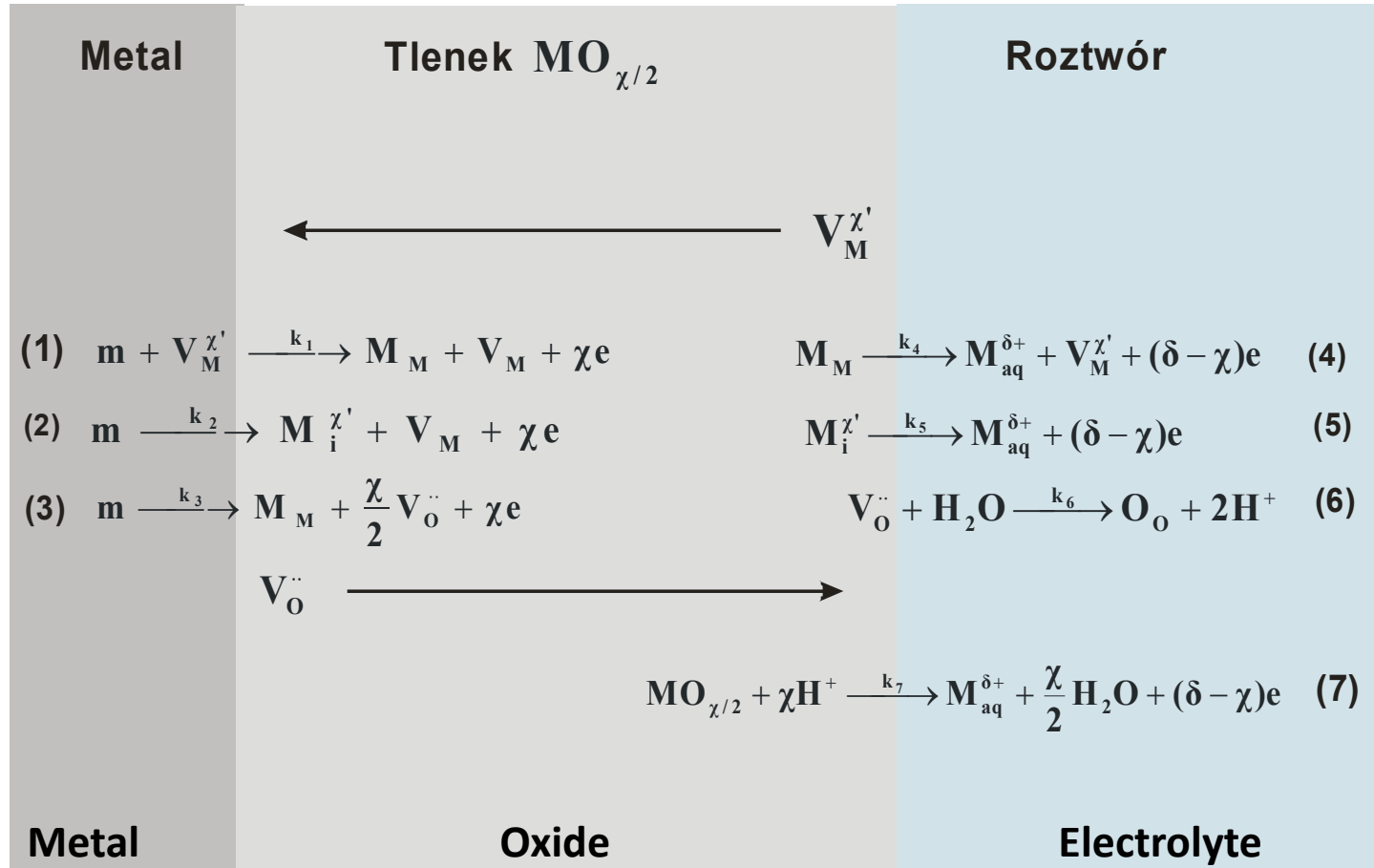
a – half jump distance

Activation energy of the ion migrating in oxide lattice without electric field

Activation energy of the ion migrating in oxide lattice with an electric field **E**

Point defects model - PDM

Metal	Tlenek $MO_{\chi/2}$	Roztwór

$$\xleftarrow{\hspace{4cm}} V_M^{\chi'}$$

(1) $\quad m + V_M^{\chi'} \xrightarrow{k_1} M_M + V_M + \chi e \qquad\qquad M_M \xrightarrow{k_4} M_{aq}^{\delta+} + V_M^{\chi'} + (\delta - \chi)e \quad$ (4)

(2) $\quad m \xrightarrow{k_2} M_i^{\chi'} + V_M + \chi e \qquad\qquad M_i^{\chi'} \xrightarrow{k_5} M_{aq}^{\delta+} + (\delta - \chi)e \quad$ (5)

(3) $\quad m \xrightarrow{k_3} M_M + \dfrac{\chi}{2} V_O^{\cdot\cdot} + \chi e \qquad\qquad V_O^{\cdot\cdot} + H_2O \xrightarrow{k_6} O_O + 2H^+ \quad$ (6)

$$V_O^{\cdot\cdot} \xrightarrow{\hspace{4cm}}$$

$$MO_{\chi/2} + \chi H^+ \xrightarrow{k_7} M_{aq}^{\delta+} + \dfrac{\chi}{2} H_2O + (\delta - \chi)e \quad (7)$$

Metal	Oxide	Electrolyte

M_M — *cation in cation site on the cation sublattice*

O_O — *oxide ion in anion site on the anion sublattice*

$M_i^{\chi+}$ — *intersitial cation*

$V_M^{\chi'}$ — *cation vacancy*

$V_O^{\cdot\cdot\cdot}$ — *oxygen (anion) vacancy*

D.D. Macdonald, Electrochimica Acta 56, 1761-1772 (2011)

Oxide growth

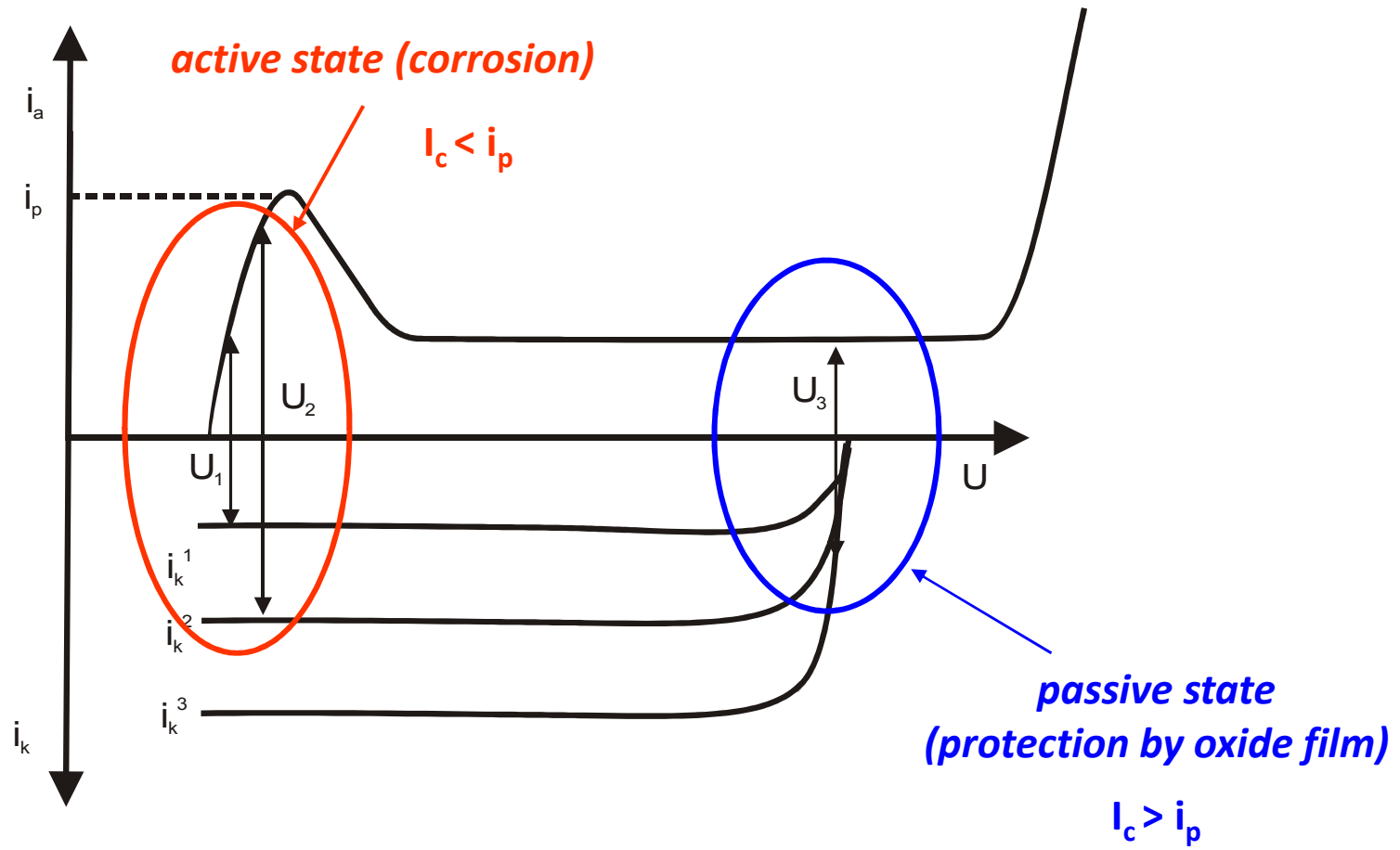| Relation describing oxide growth	Charge q_w necessary to oxide growth in the time t	Current density i_w necessary to oxide growth in the time t	Slope	Mechanism determining oxide growth
parabolic	$q_w = k_p \cdot t^{\frac{1}{2}}$	$i_w = \dfrac{1}{2} k_p \cdot t^{-\frac{1}{2}}$	$-\dfrac{1}{2}$	diffusion
logarithmic	$q_w = k_l' + k_l \cdot \ln t$	$i_w = k_l \cdot t^{-1}$	-1	exchange place, high field migration
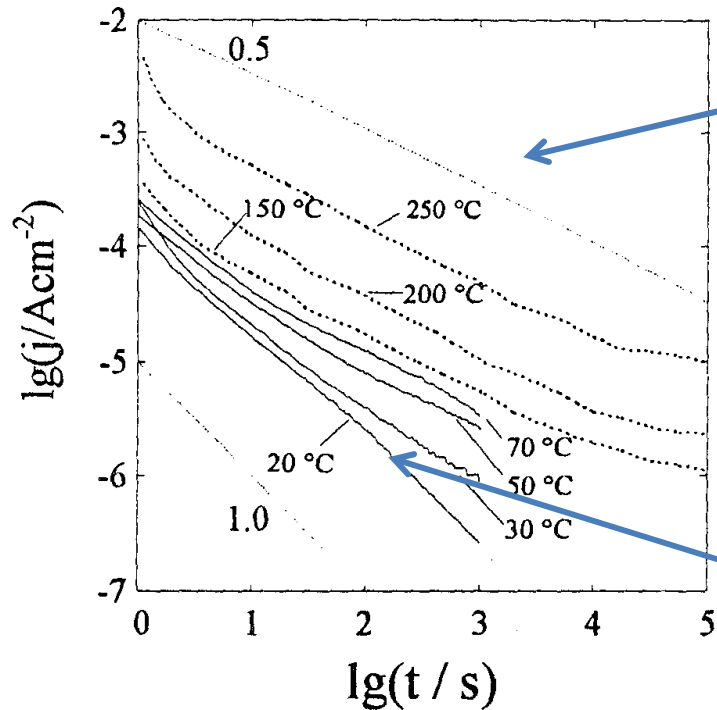
Growth of oxide film on iron surface in aqueous solutions, pH 7.4 – 7.8

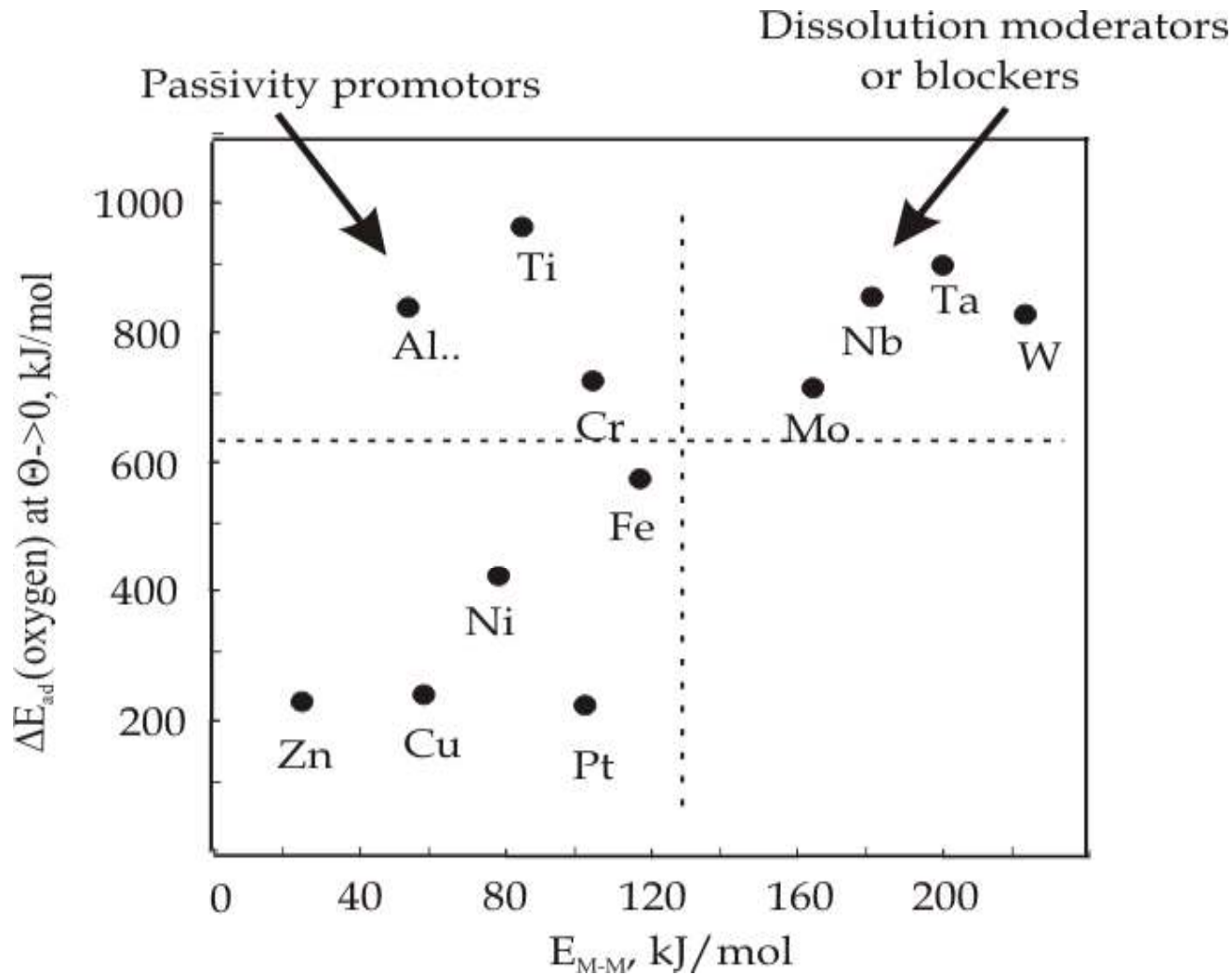K.E. Heusler, B. Kusian, D. McPhail: Ber. Bunsenges. Phys. Chem. 94, 1443 (1990)

Effect of oxidant concentration on spontaneous passivation of metal

Passivity of metallic alloys

Passivity promoters and dissolution moderators according to the synergy between the energy of the metal-metal bonds and heat of adsorption of oxygen
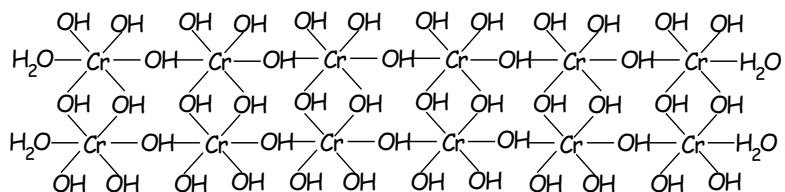
P. Marcus: Corr.Sci. 36, 2155 (1994)

Effect of chemical composition on passive behaviour of the alloy

% Cr	% Ni
3,54	9,85
7,45	9,50
11,74	9,12
16,10	8,60
19,20	8,32
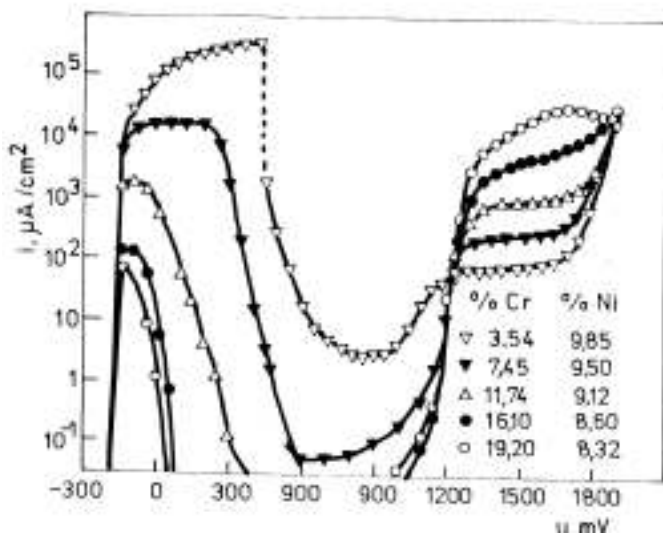
Stationary polarization curves of austenitic Fe-Cr-Ni alloys in 1M H_2SO_4
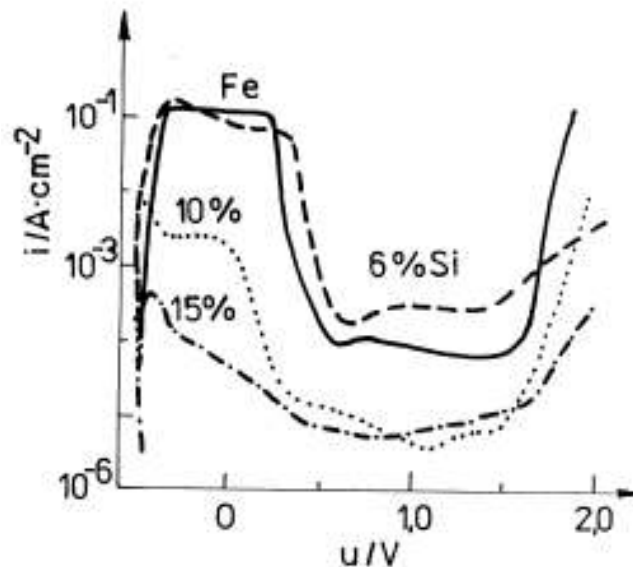
Stationary polarization curves of Fe-Si alloys in 1M H_2SO_4

Model of passive film on pure chromium

% Cr	Structure of passive film	thickness A^0
0	well oriented spinel	36
5	well oriented spinel	27
12	weak oriented spinel	21
19	mainly amorphous	19

Effect of chromium on the structure of passive film on Fe-Cr alloys in neutral aqueous solutions
J.Kruger in Passivity of Metals, ed.by Electroche. Soc. Inc. Princetown ,N. Jersey 1978
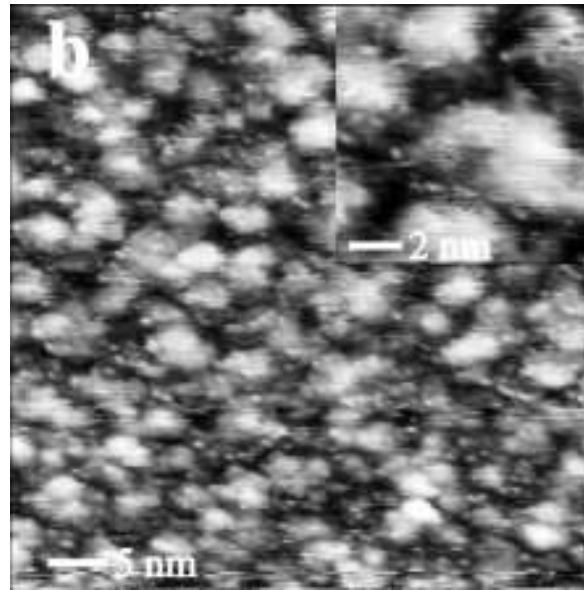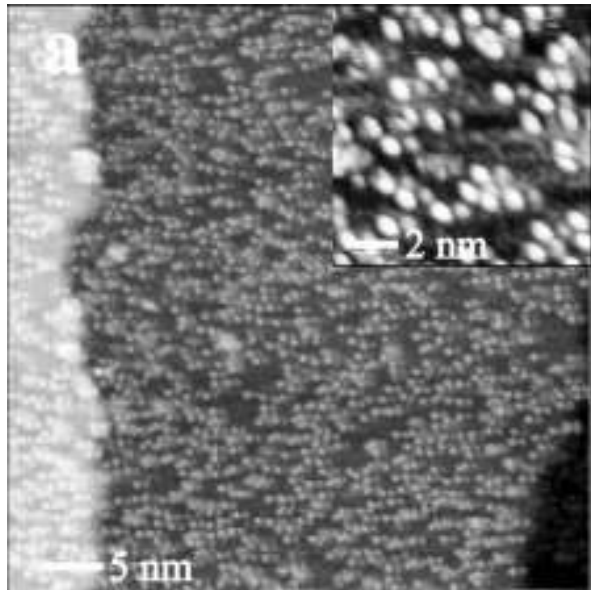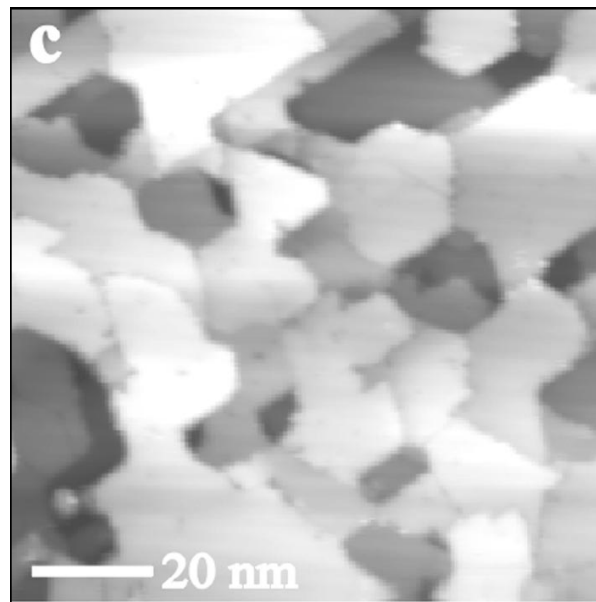
Oxide growth (Cr/Cr$_2$O$_3$)

STM topographic images of the Cr(110) substrate after exposure to 0.75 L (a) and 2.25 L (b) of oxygen at 300 K.

27 C

O$_2$
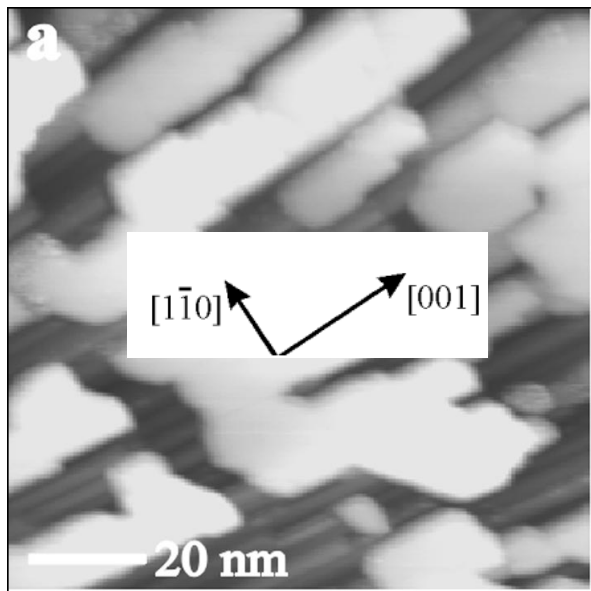
STM topographic images of the oxide film formed by exposure of Cr(110) to 3.4 L (a), 7.5 L (b) and 11.3 L (c) of oxygen at 625 K and subsequent annealing at 925 K.

[1$\bar{1}$0]   [001]

352 C + 652C annealing

V. Maurice, S. Cadot, P. Marcus, Surface Science 458 (2000) 195–215

Oxide growth (Cr/Cr$_2$O$_3$)

At 300 K, a granular and non-crystalline oxide is formed, which grows with a constant ~Cr$_2$O$_3$ stoichiometry up to a limiting thickness of 0.9 nm. The film is hydrated with a water content of 10–20%, which decreases upon annealing. Nuclei of oxide with a lateral dimension of ~0.7 nm and a height of ~0.2 nm have been observed in the nucleation stage. These nuclei grow predominantly laterally and coalesce to fully cover the substrate surface prior to the thickening stage.
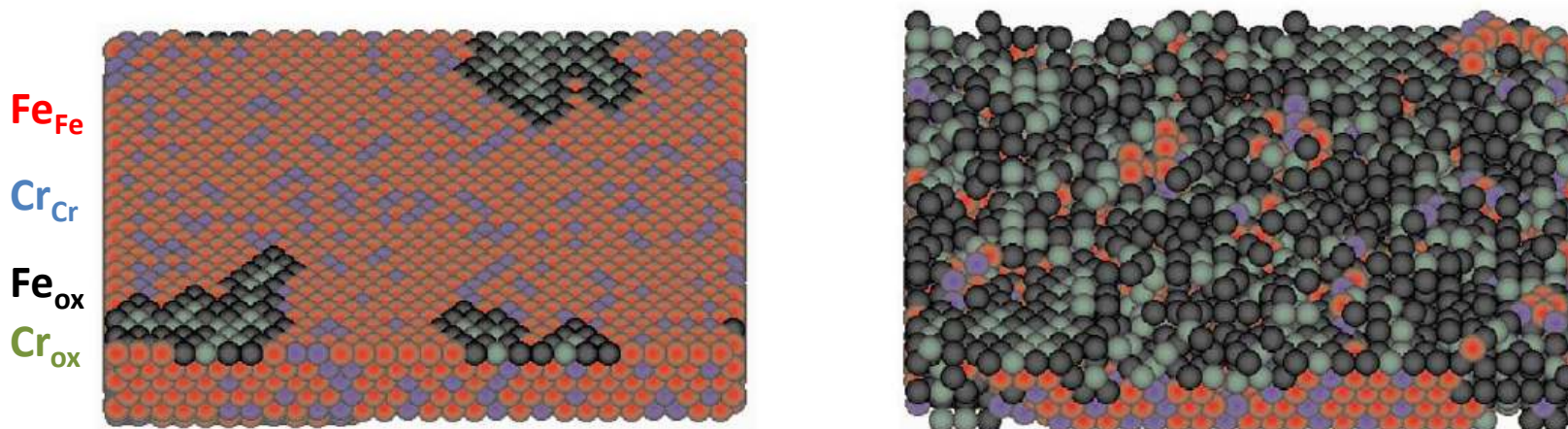
At 625 K, a first stage of oxygen adsorption is observed in which stripes 1.5–2.3 nm wide and parallel to the Cr[001] direction are observed after annealing in UHV. They correspond to narrow segments of mixed and close-packed planes of O atoms and ions having a geometry and orientation similar to those of the anions planes in the oxide crystals. Rows of adatoms, possibly Cr^{3+} ions of oxide nuclei, are observed above the stripes. Thickening at 625 K leads to the formation of a non-crystalline oxide, which grows up to a limiting thickness of 4.6 nm. The presence of Cr3+ vacancies related to a significant cation transport through the oxide film in this temperature regime is detected. After UHV annealing at 825 or 925 K, the film is anhydrous. The Cr3+ vacancies are accumulated at the metal/oxide film interface. The film crystallizes in epitaxy with the substrate in the following orientation: α-Cr$_2$O$_3$(0001) || Cr(110) and α -Cr$_2$O$_3$[213:0] || Cr[001].

V. Maurice, S. Cadot, P. Marcus, Surface Science 458 (2000) 195–215

Passivation of alloys

Effect of the chromium content of the alloy on the simulation of passivation (size of the model: $80 \times 80 \times 60 \text{ Å}^3$)

Chromium concentration in the alloy (%)	Number of planes in which corrosion has propagated (mean)	Probability of passivation	Chromium concentration in the passive layer (%)	Roughness
12	Perforated	0	–	9.3
13	Perforated	0	–	8.9
14	Perforated	0	–	8.5
15	Perforated	0	–	7.7
16	26	0.375	24	7
17	20	0.75	24.5	5.8
18	15	1	25.2	5.5
22	10	1	30.6	3.6

Fe_{Fe}

Cr_{Cr}

Fe_{ox}

Cr_{ox}

Simulation of the dissolution and passivation of Fe-22%Cr alloy at the beginning of simulation process (a) and after simulation (b)

M.Legrand, B.Diawara, J.-J.Legrende, Ph.Marcus, Corr.Sci, 44, 773-790 (2002)